



Recent advances in RV Tauri stars

SUNETRA GIRIDHAR

Indian Institute of Astrophysics, Bengaluru 560034, India.
E-mail: giridhar@iiap.res.in

MS received 3 September 2020; accepted 20 November 2020

Abstract. The availability of multi-wavelength observations and parallaxes from the space missions and very comprehensive models of AGB evolution that include the accretion of matter from the circumbinary disc have strongly impacted our understanding of these enigmatic objects. The important developments made in the recent times are summarized here. The revised estimates of luminosities (derived from better-defined Spectral Energy Distributions (SEDs) and new distances from Gaia DR2) further support the opinion that RV Tauri stars contain a mixture of post-AGB stars and post-RGB stars. Their locations in HR diagram also indicate that the instability strip (IS) of RV Tauri stars have a broader extension in the cooler edge than that of classical Cepheids. A new P–L relation has been calibrated for the galactic Cepheids which have a steeper slope than that derived for the Population II Cepheids and RV Tauri stars in Magellanic clouds. The most significant chemical peculiarity exhibited by RV Tauri stars and other post-AGB stars is the selective depletion of refractory elements that correlates with their condensation temperatures. A large range in the size of depletion as well as in the shapes of the depletion curves has been observed. Earlier models to explain this effect were mostly qualitative. Recent investigators model these depletions using evolutionary codes (e.g. MESA) to evolve stars in the post-AGB phase, while including accretion of metal-poor gas from circumbinary disc. These authors model the accretion rate onto a the binary post-AGB star from a viscously evolving disc for a range of initial accretion rates and disc masses. It is reported that large initial accretion rates and disc masses are required to explain the large depletion and saturated depletion curve that could extend the evolution time of post-AGB star. It is also proposed that the unsaturated depletion curve (with a plateau) are likely to be caused by post-RGB stars.

Keywords. RV Tauri stars—luminosities—abundances.

1. Introduction

The prototype RV Tauri was discovered in 1905 by Lyndia Ceraski using photographic photometry. A follow-up by Sears and Haynes (1908) showed that the RV Tauri light curve contained two alternating deep and shallow minima, and the depths of the light minima were modulated in a irregular way. van der Bilt (1916) carried out a detailed analysis of RV Tauri photometry and found similarities between them and

Cepheid variables. It is now well known that both these groups of variables are pulsating stars.

1.1 Photometric characteristics

The photometric periods of RV Tauri stars range from 30 to 150 days, while the amplitude of variations could be as large as 4 magnitudes in V. The formal period is defined as time between the two successive deep minima, whereas the time between the two successive minima is called the fundamental period. The light variations are cyclic (not strictly periodic) and depths of light minima are also not constant. These objects are divided into two photometric classes: RVa stars are those having stable maximum

This article is part of the Topical Collection: Chemical elements in the Universe: Origin and evolution

magnitude and RVb class stars are those that have a long periodic change in maximum light.

1.2 Spectroscopic classification

The seminal work by Preston *et al.* (1963) covering a large sample of RV Tauri stars led to the following spectral classifications. They are classified as A, B, or C depending upon both their temperatures, the presence and strength of specific molecular lines in their spectra.

Class A stars are cooler stars of spectral types G and K at maximum, but show irregularities in CN band strengths and strong bands of TiO appear near minimum light.

Class B stars are hotter stars of spectral type F, some having weaker metal lines. But these stars have abnormally strong CH and CN bands.

Class C stars have temperatures similar to class B but display weak CH, CN Bands, weak metal lines and high radial velocities similar to Population II objects. Wallerstein (2002) pointed out that the proper motions of the class A and B stars show that they belong to the thick disk population of the Milky Way. The RVC RV Tauri stars are found in globular clusters further supporting the suggestion that they are Population II objects. We had studied two galactic RV C stars: V453 Oph and V820 Cen (Giridhar *et al.* 2000; Rao & Giridhar 2014); both are metal-poor stars with high radial velocities.

2. Evolutionary status of RV Tauri stars

Due to their high luminosities and the presence of IR excess in many of them, RV Tauri stars were classified as post-AGB objects crossing the instability strip (Lloyd Evans 1985; Jura 1986). The distances (hence luminosities) of pulsating stars can be determined by Period–Luminosity (P–L) relation. The early calibration of P–L relation for galactic RV Tauri stars suffered from paucity of objects with well-determined distances. The calibration of P–L relation for type II Cepheids in the LMC by Alcock *et al.* (1998) confirmed high luminosities of these objects. Later large-scale surveys of LMC and SMC post-AGB stars (Kamath *et al.* 2015, 2016) indicated them to be more heterogeneous objects including post-RGB objects.

Based on the shape of their SEDs particularly in IR, they were classified into different group by Gezer *et al.* (2015). The first group contains stars that display SEDs with a broad IR excess starting in the near

IR region, indicating the presence of hot dust near the star. These stars were called disc sources by Gezer *et al.* (2015). The second group displays doubled-peaked SEDs where the first peak corresponds to the stellar photospheric flux and the second peak at mid-infrared is caused by IR emission of an expanding dusty envelope. These authors referred them as shell sources. Besides these two groups, Gezer *et al.* (2015) found a large fraction of RV Tauri stars with no IR excess or showing only uncertain excess. Gezer *et al.* (2015) find clear correlation between the disc sources and binarity. Most of the RVb stars are disc-type sources.

Manick *et al.* (2017) have calibrated the Period Luminosity Color (PLC) relation for RV Tauri stars in the Magellanic clouds. Manick *et al.* (2018) have studied the evolutionary status of RV Tauri stars in LMC and SMC. Using the luminosity derived from PLC relation and those derived from SEDs they discuss their location in Hertzsprung–Russel diagram. These authors further reiterate that RV Tauris contain post-AGB and post-RGB stars.

Bodi and Kiss (2019) have compiled the photometric and spectroscopic data for galactic RV Tauri stars to calibrate their P–L relation. These authors used photometric measurements, extinction and bolometric correction to derive luminosities and absolute magnitudes of the sample stars. Distances were determined using Gaia DR2 to derive the luminosities of these objects. The systematic error in Gaia DR2 parallaxes were corrected by using the procedure proposed by Astraatmadija and Bailer-Jones (2016). The extinction A_V by the authors were taken from the combination of 3D reddening maps by Marshall *et al.* (2006), Green *et al.* (2015) and Drimmel *et al.* (2003) as implemented in the Python package of mw dust (Bovy *et al.* 2016). Bolometric corrections were linearly interpolated from T_{eff} , $\log g$ and $[\text{Fe}/\text{H}]$ and A_V in the MIST/CAK grid (Conroy *et al.* 2019). T_{eff} , $\log g$ and $[\text{Fe}/\text{H}]$ were taken from the literature or the Gaia archive.

In the empirical Hertzsprung–Russell diagram generated by these authors also contains the post-AGB evolutionary tracks for stars in mass range 1.0 to 4.0 M_{\odot} for $z=0.01$ and 0.014 by Bertolami (2016) and Charbonnel *et al.* (2017) respectively. The location of the tip of the RGB for 1 and 4 M_{\odot} is also indicated. From their location in the H–R diagram, it is apparent that the RV Tauri stars with near IR excess (disk type) and RVb type are high-luminosity objects with luminosities from 700 to 5500 L_{\odot} . It is proposed that these dusty objects that have higher luminosities than 1 M_{\odot}

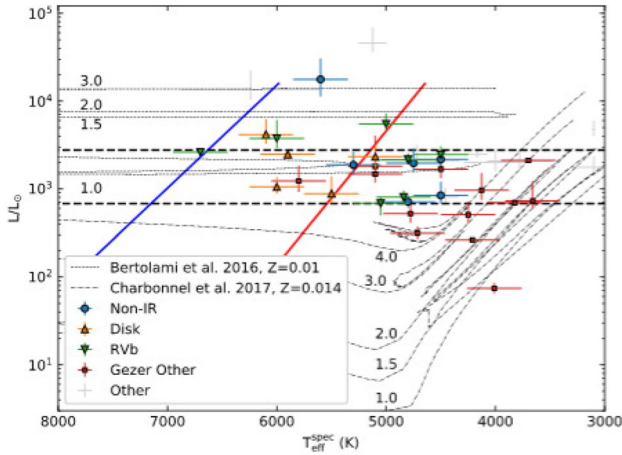


Figure 1. Empirical Hertzsprung–Russell diagram for galactic RV Tauri stars. Blue points are stars with no IR excess, orange triangles stars with detectable disk, green downward triangles are RVb variables, red points are other stars. These are taken from Gezer *et al.* (2015). Gray crosses are other stars taken from literature. The blue and red diagonal lines indicate the edges of the classical instability strip, adopted from Christine-Dalsgaard (2003). The figure also contains evolutionary tracks for two metallicities. The black horizontal dashed lines indicate the tip of RGB of $1 M_{\odot}$ (upper) and $4 M_{\odot}$ (lower) models. This figure is taken from a paper titled ‘Physical Properties of Galactic RV Tauri Stars from Gaia DR2 Data’ by Bodi and Kiss (2019), *ApJ*, 872, 608–617, and has been reproduced with permissions from authors and AAS.

Tip of the Red Giant Branch (TRGB) (upper horizontal line in the Figure 1) are probably post-AGB stars with initial mass higher than $1 M_{\odot}$. These authors suggest that lower luminosity objects are probable post-AGB stars if they have initial mass between about 2 to $4 M_{\odot}$. Otherwise, they most likely were formed from lower-mass binary post-RGB progenitors. Further, lower-luminosity objects are likely post-RGB binary stars with lower progenitor masses. A significant number of non-IR, with uncertain IR excess and RVb stars, are outside the red limit of the instability strip. These authors ascribe it to the structural differences between classical Cepheids and RV Tauri stars or the difference between the excitation mechanism.

3. Period–Luminosity relation

The period–luminosity relation derived using Magellanic cloud data for Population II Cepheids and later for RV Tauri stars have been used in the past to estimate the luminosities of galactic RV Tauri stars.

The period–luminosity relation for galactic RV Tauri stars calibrated by Bodi and Kiss (2019) using high-confidence data on 17 RV Tauri star is very important in this context. A linear equation fitted to the logarithmic quantities of the sample stars in period range 40–100 days with a 2σ clipping is given below.

$$\text{Log}L/L_{\odot} = 2.62^{+0.05}_{-0.01} \text{Log} P - 1.52^{+0.07}_{-0.22} \quad (1)$$

The two outliers from the data were excluded. The slope of this relation is steeper than that of P–L relations derived for Population II Cepheids and RV Tauri stars in the Magellanic cloud by Groenewegen and Jurkovic (2017).

In addition to the period–luminosity relation, Bodi and Kiss (2019) have also determined period–absolute magnitude relation. This relation is very important since it allows easy comparison with older studies as more data in the V band is available in literature.

$$M_V = -7.36^{+0.07}_{-0.38} \text{Log} P + 10.21^{+0.98}_{-0.33} \quad (2)$$

Here 3 outliers out of the 17 sample stars were excluded.

4. Chemical composition of RV Tauri stars

Although chemical composition studies of RV Tauri were undertaken with the hope of getting insight into AGB nucleosynthesis and mixing since these are post-AGB objects, the outcome was, however, quite unexpected. Only two galactic RVC objects (V 453 Oph and V820 Cen) exhibited mild s-process enhancement with extremely low carbon abundances (Rao & Giridhar 2014). In LMC and SMC a few RV Tauri stars with significant enhancement of carbon and s-process elements have been reported (Reyniers *et al.* 2007; Van Aarle *et al.* 2013). Even among the well-studied post-AGB stars, the fraction of stars showing the signature of AGB nucleosynthesis is not that large. A compilation of the RV Tauri stars and other post-AGB stars showing different kinds of chemical peculiarities is presented by Rao *et al.* (2012, 2014).

4.1 Abundance peculiarities in RV Tauri and other post-AGB stars

A large fraction of RV Tauri and post-AGB stars exhibit systematic under-abundances of refractive elements which shows strong dependence on their condensation temperatures. The low-condensation-temperature elements like C,N,O, S and Zn are not

affected, while high-condensation-temperature elements like Sc, Ti and Fe are heavily depleted. A strong signature of this effect was reported for BD+39°4926 (Luck & Bond 1984), HR 4049 (Lambert *et al.* 1988), HD 52961 (Waelkens *et al.* 1991), etc. In RV Tauri stars the first detection of this systematic under-abundances of refractive elements was reported for IW Car by Giridhar *et al.* (1994). It is shown by Kameswara Rao & Reddy (2005) that in a few RV Tauri stars like CE Vir, EQ Cas and IRAS 18386-1253, the elemental depletion show significant dependence on the first ionization potential (FIP) of the element. These authors suggest that the stellar wind preferentially picks up ions over neutral atoms. At the upper atmospheric layers, the elements with low FIP will be present as ionized species while those with high FIP will remain neutral.

In their study of λ Boo stars, similar depletions were reported by Venn & Lambert (1990), who pointed out the resemblance of their abundance pattern to the interstellar gas in which metals are depleted through fractionation in the interstellar gas. Bond (1991) suggested that the extreme metal-deficiency of HR 4049 like objects could be caused by the selective removal of metals through grain formation. To explain these abundance peculiarities, Mathis & Lamers (1992) proposed two scenarios: capture by the presently visible post-AGB stars of the depleted gas from the binary companion, or rapid termination of a vigorous stellar wind in a single star so that the grains are blown outwards (hence lost) resulting in a photosphere devoid of these grain forming elements.

An alternating scenario was proposed by Waters *et al.* (1992) based upon slow accretion from the circumstellar or circum-system disk. This scheme provides for this effect to operate without any restriction on the nature of the binary companion. These authors explain that in their scenario a circum-system disk may develop whether the companion is a low mass star or a white dwarf and accretion from circum-system disk can take place after strong AGB wind has stopped allowing for more mass to be accreted. Further progress was made through the detection of many more post-AGB stars (including RV Tauri stars) showing various degrees of depletions as reported by Van Winckel (1995, 1997, 2003), Van Winckel *et al.* (2012), Giridhar *et al.* (1994, 1998, 2000, 2005), Gonzalez *et al.* (1997a, 1997b), Maas *et al.* (2005) and many others.

The enlarged sample highlighted the importance of boundary conditions like minimum temperature, minimum metallicity, binarity and the shape of SED.

Van Winckel and his group, through their numerous papers, reported binary companions in many post-AGB stars including RV Tauri stars; see, for example, Van Winckel (2009) and more recently Manick *et al.* (2017). Van Winckel and his group also reported the evidence for the presence of dust in a flattened geometry. Gezer *et al.* (2015), who studied the SEDs for a large number of post-AGB stars and RV Tauri stars, found a close link between the observed depletion and disc-type SEDs. Besides this, disc-type post-AGB stars are more common among post-AGB stars. A study of post-AGB stars in Magellanic clouds by Kamath *et al.* (2015, 2016) also report that disc-type post-AGB outnumber those with shell-type SEDs.

The CO survey by Bujarrabal *et al.* (2013) of these objects has shown their gas structure to be in Keplerian rotation based on the narrow emission profiles of the CO rotational excited lines. The near IR milli-arcsec-scale imaging of several post-AGB binaries has resulted in well-resolved images of these binary systems surrounded by hot circumbinary dust. A detailed view of a dusty circumstellar disk around IRAS 08533-4431 system is obtained by Hillen *et al.* (2016).

5. Observed depletion patterns and possible interpretation

Although the observed abundance pattern has a dependence on T_c (condensation temperature), it is not a simple linear relation but a plethora of different depletion patterns is observed depending upon the extent (size) of the depletion and the turn-off temperature, and for some post-AGB stars, a different depletion profile is caused by the fact the under-abundances of all refractory elements is the nearly same although they have different T_c s. The example of this case is GZ Nor, as shown in Figure 2.

The size of depletion can be measured through ratio of the most depleted element (Ti,Sc) to non-depleted volatile element (S,Zn). The ratio is always written as compared to the solar composition, e.g. [S/Ti] or [Zn/Ti]. The second factor is the turn-off temperature that defines the limit for which elements with higher T_c become depleted. As shown in Figure 2, for GZ Nor and IRAS 11472-8000, T_c is around 800–1000K, but for IRAS09144-4933, it is 1500K.

A very detailed systematic investigation of post-AGB (including RV Tauri) stars has been carried out

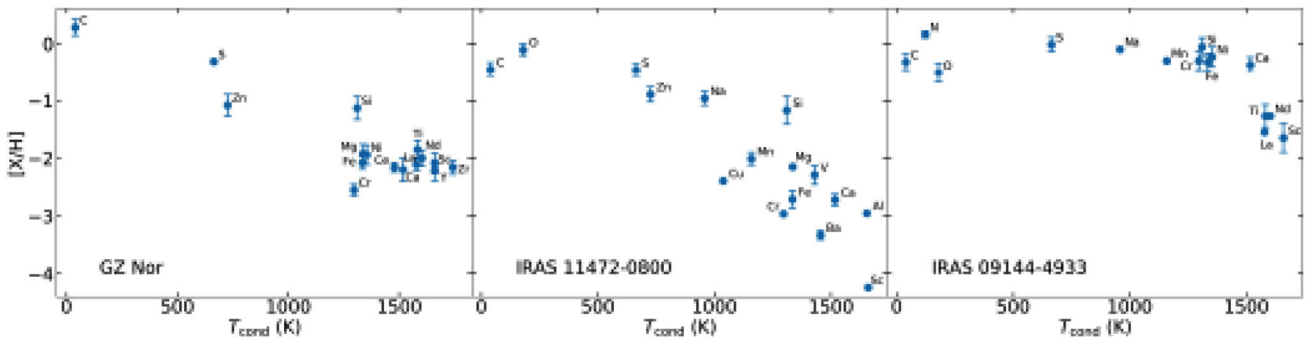


Figure 2. The depletion pattern for three selected stars illustrating the diversion in the shape of their abundance pattern despite their dependence on T_c is present. The abundances are plotted with respect to solar composition. The figure has been taken from Oomen *et al.* (2019), *A&A*, 629A,490, reproduced with permission ©ESO.

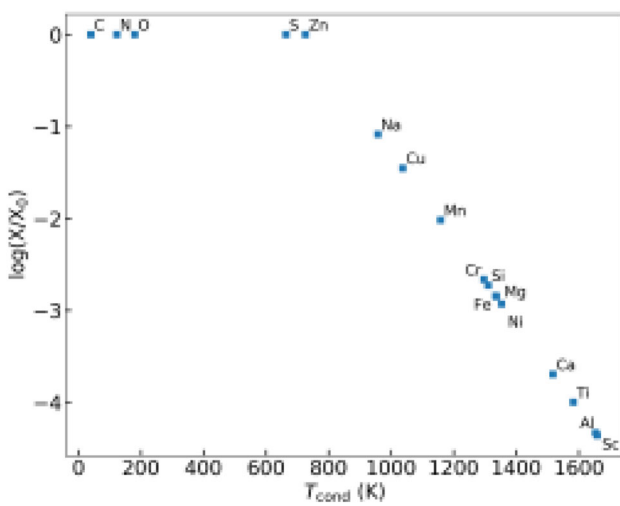


Figure 3. An estimate of chemical abundances of accreted gas is based upon the abundances of one of the most depleted observed post-AGB stars IRAS 11472-0800 is plotted as a function of T_c . The figure has been taken from Oomen *et al.* (2019), *A&A*, 629A,490, reproduced with permission ©ESO.

by Oomen *et al.* (2019). These authors analyzed a large sample of post-AGB stars showing different depletion patterns and developed an evolutionary model that included re-accretion of gas from a dusty disc in post-AGB stars.

6. Gas dilution model

As the gas from circumstellar disk is accreted onto the star, the gas mixes with the convective outer layers. Since the chemical composition of the accreted gas is different from that of the star, the chemical composition of the photosphere will gradually change as

more gas is accreted, which results in the observed depletion pattern of post-AGB stars. In order to determine the chemical composition of the accreted material, Oomen *et al.* (2019) used the chemical composition of one of the most depleted stars, IRAS 11472-8000 (Van Winckel 2012), as the reference. This is shown Figure 3. Since the abundance of the most depleted element Sc is around -4 dex relative to the solar, the accreted abundance of Ti is taken as -4 dex and the abundance of volatile element Zn is kept at 0.0 since this element does not show under-abundance in most metal-poor stars. The photospheric abundance of the post-AGB star suffer dilution as the star accretes metal-poor gas from the circumbinary disc. Figure 4 shows the resulting composition after the dilution by factors 2, 100 and 1000. When the amount of gas that has been accreted is equal to the initial mass of the mixture, the refractory elements would show decrease by factor 2 (0.3 dex). For dilution by a factor of 100, the large number of elements that have mild under-abundances (-2.0 dex) in accreted gas become saturated and converge to the abundance of the accreted gas while those at high T_c are still not converged. The abundance profile thus has plateau shape. For dilution of 10000, even the elements with highest-condensation-temperature stars converge to their accretion abundances giving a saturated profile similar to that given in the third panel of Figure 3.

6.1 Limitation of gas dilution model

The simple gas dilution model can explain the abundance profile like unsaturated profile with a plateau and saturated profiles seen in many post-AGB stars. However, the observed diversity regarding the

maximum depletion value and the turn-off temperature cannot be reproduced. This is very obvious from the pattern observed for IRAS 09144-4933. This indicates that the chemical composition of the accreted gas can differ from star to star. Oomen *et al.* (2019) undertook the task of understanding these abundance profiles in post-AGB stars in greater detail by computing a set of detailed stellar evolution models while including accretion of depleted gas. These models were then compared to the observed post-AGB stars of similar masses.

Based upon earlier findings, e.g by Vassiliadis & Wood (1994), it is known that the main property of a post-AGB star that determines its luminosity is the core mass; hence, one can use the luminosity of the stars to estimate its current mass. By separating the stars into several bins, these authors carried out the evolutionary calculations using MESA code to evolve stars in these mass bins to post-AGB phase. These authors modelled the accretion rate onto binary from viscously evolving disc for a range of initial accretion rates and disc masses. These authors report that accretion rate as large as or greater than $3 \times 10^{-7} M_{\odot}/\text{yr}$ and large initial disc masses of $10^{-2} M_{\odot}$ are required to explain the observed depletion patterns of post-AGB stars. These authors also suggest that the high accretion rates can extend evolutionary time-scales of post-AGB stars by a factor between 2 and 5.

The agreement between the depletion pattern computed using the accretion model and the observed abundances is shown in Figure 5. The two stars chosen have similar turn-off temperatures as that of the accretion model (800K). The top panel shows the comparison for EP Lyr, which has a plateau profile, while the bottom panel shows the data for CC Lyr,

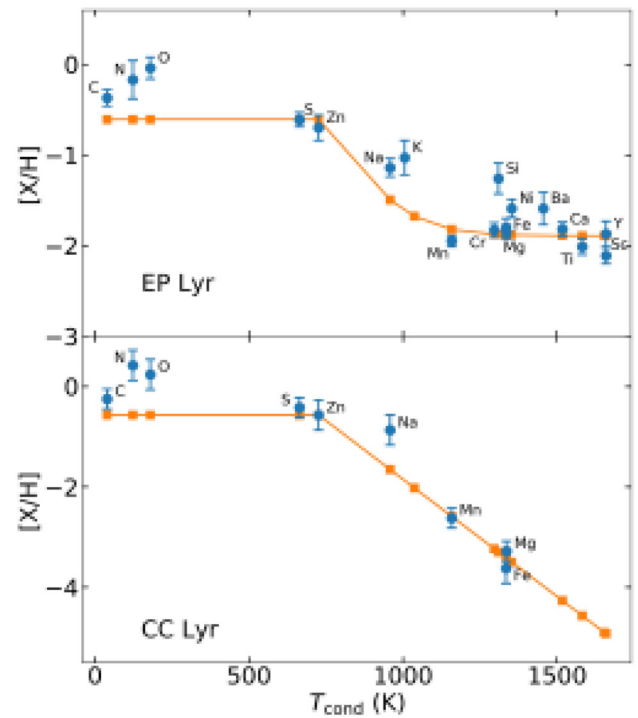


Figure 5. The comparison between the observed depletion pattern and the best fitting model for a plateau-type profile (top EP Lyr) and a saturated-type profile (bottom CC Lyr). Observed abundances of elements are given as blue circles, while abundances from the accretion model are presented by orange squares. The evolutionary model uses the abundances of accreted gas as those given Figure 3. The figure has been taken from Oomen *et al.* (2019), *A&A*, 629A, 490, reproduced with permission ©ESO.

which has a saturated profile. The abundances of the models shown in Figure 5 are a snapshot of the abundances in the outer layer of the MESA models at the observed effective temperatures of EP Lyr and CC

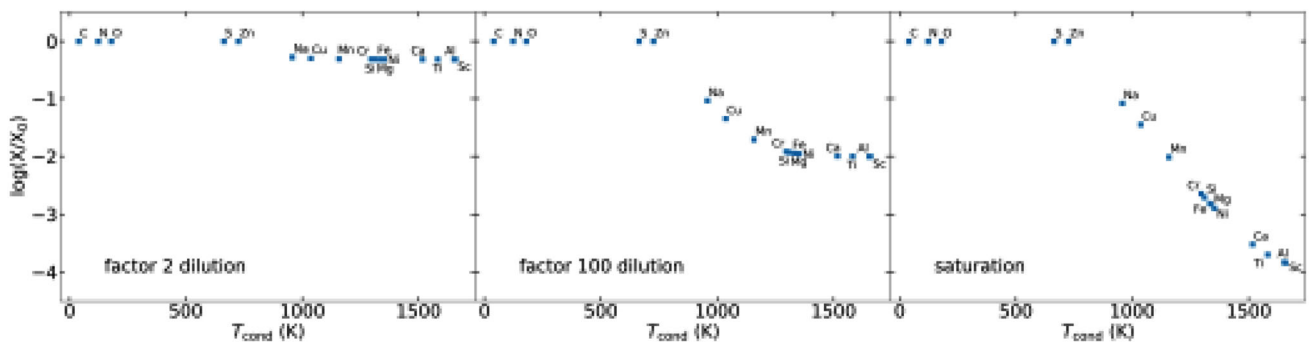


Figure 4. The chemical composition of a gas mixture after dilution of a solar composition gas with abundances from Figure 3. The left panel shows the composition after dilution by a factor of 2. In the middle and right column the same with dilution factors of 100 and 10 000 respectively. The figure has been taken from Oomen *et al.* (2019), *A&A*, 629A, 490, reproduced with permission ©ESO.

Lyr. Oomen *et al.* (2019) used a $0.55 M_{\odot}$ post-AGB model starting accretion at 5000K with initial mass-loss rate of $5 \times 10^{-7} M_{\odot}/\text{yr}$ and disc mass M_d of $10^{-3} M_{\odot}$ taken at 6200K. For CC Lyr the best fit was obtained for $0.40 M_{\odot}$ post-RGB star starting accretion at 4000K with initial mass-loss rate of $5 \times 10^{-8} M_{\odot}/\text{yr}$ and disc mass M_d of $10^{-2} M_{\odot}$ taken at 6250K. These authors suggest that the differences between post-RGB stars and post-AGB stars are caused by large differences in luminosities and hence evolutionary timescales. Because of the slow evolution of post-RGB stars, it is expected that these stars are much more likely to show an unsaturated plateau-like profile in their abundance pattern, although observationally only 20% of the post-RGB stars show the plateau pattern. It is also reported that the post-RGB star can become mildly or moderately depleted at relatively low T_{eff} ($< 5000\text{K}$), while more massive post-AGB stars evolve too fast and can only become depleted at temperature of 6000K or larger. This is corroborated by the observations of several depleted post-RGB stars at low T_{eff} and lack of depleted post-AGB stars at T_{eff} less than 6000K.

7. Summary

- Comprehensive study of RV Tauris in galactic sample as well as in LMC and SMC has resulted in improved calibrations of PL relations for RV Tauri in these systems. Improved estimates of luminosities have further reiterated that RV Tauri are a mixture of post-AGB stars and post-RGB stars.
- The number of binary detection in post-AGB stars and RV Tauri stars have grown manifold. The orbital parameters and masses are important inputs to develop models to explain the observed depletions. It is indicated that wide binaries are more likely to show this effect.
- A study of their circum-binary shell through IR interferometry for certain systems, e.g. IRAS 08544-4431, by Hillen *et al.* (2016) have helped in constraining the parameters for these shells.
- Comprehensive evolutionary models including re-accretion of gas from a dusty disc in post-AGB stars have been developed that can quantitatively explain the observed depletion patterns in post-AGB stars including RV Tauri stars. While a commendable beginning is made in developing such models to explain the

observed depletion patterns, many parameters like stellar wind prescription, accretion rate and mixing process need to be formulated better.

Notwithstanding the progress made, much work needs to be done in many areas towards better understanding of evolutionary status of these objects. While RV Tauri stars were originally considered post-AGB stars, it is becoming increasingly apparent that they are a mixed lot, comprising post-AGB and post-RGB stars. With increased detection of binarity, the impact of binarity on their evolutions is being explored but models require refinement. An extended samples of RV Tauri stars with binary companions and high-spatial-resolution interferometry (particularly in infrared) of these objects would give valuable information towards developing more comprehensive models to explain the observed peculiar abundances of these objects.

Although a recent attempt has been made to calibrate the P–L relation for galactic RV Tauri stars based on Gaia DR2, the binarity may introduce errors in the distance hence luminosity estimates. The calculations based Gaia DR3 might improve these estimates.

For some reason, no progress has been made towards developing detailed models to explain the RV Tauri-like pulsation in the last few decades, the last papers being those of Takeuti and Peterson (1983) and Fokin (1994) to best of our knowledge.

Acknowledgements

The author thanks the organizers of the meeting for the invitation to deliver this talk. The author also thanks the anonymous referee whose comments have improved the article.

References

- Alcock, C., Allsman, R.A., Alves, D.R. *et al.* 1998, AJ, 115, 1921
- Astraatmadija, T.L., Bailer-Jones, C.A.L., 2016, ApJ, 832, 137
- Bertolami, M.M., 2016, A&A, 588, 25
- Bodi, A. and Kiss, L.L., 2019, ApJ, 972, 60
- Bond, H.E., 1991, Proc. IAU Symp. 145, Evolution of stars: the photospheric abundance connection, 341
- Bovy, J., Rix, H.-W., Green, G.M., Schlafly, E.F., *et al.* 2016, ApJ, 818, 130
- Bujarrabal, V., Alcolea, J., van Winckel, H., *et al.* 2013, A&A, 557, 104

- Ceraski, W., 1905, A.N., 168, 29
- Charbonnel, C., Decressin, T., Lagarde, N. *et al.* 2017, A&A, 605, 102
- Christine-Dalsgaard, J., 2003, Lecture Notes on Stellar Oscillations, Aarhus University, May 2003, 5th edition (<http://astro.phys.au.uk/jcd/oscilnotes>)
- Drimmel, R., Cabrera-Lavers, A., Lopez-Corredoira, M., 2003, A&A, 409, 205
- Fokin, A.B., 1994, A&A, 292, 133
- Gezer, I., Van Winckel, H., Bozkurt, Z., De Smelt, K., Kamath, D., *et al.* 2015, MNRAS, 453, 133
- Giridhar, S., Kameswara Rao, N.K., Lambert, D.L., 1994, ApJ, 437, 476
- Giridhar, S., Lambert, D.L., Gonzalez, G., 1998, ApJ, 509, 366
- Giridhar, S., Lambert, D.L., Gonzalez, G., 2000, ApJ, 531, 521
- Giridhar, S., Lambert, D.L., Reddy, B.E., Gonzalez, G., Yong, D., 2005, ApJ, 627, 432
- Gonzalez, G., Giridhar, S., Lambert, D.L., Giridhar, S., 1997a, ApJ, 481, 452
- Gonzalez, G., Giridhar, S., Lambert, D.L., Giridhar, S., 1997b, ApJ, 479, 427
- Green, G.M., Schlafly, E.F., Finkbeiner, D.P., *et al.* 2015, ApJ, 810, 25
- Groenewegen, M.A.T., Jurkovic, M., 2017, A&A, 604, 29
- Hillen, M., Kluska, J., Le Bouquin, J.-B., *et al.* 2016, A&A, 588, L1
- Jura, M., 1986, ApJ, 309, 732
- Kamath, D., Wood, P.R., Van Winckel, H. 2015, MNRAS, 454, 1468
- Kamath, D., Wood, P.R., Van Winckel, H. and Nie, J.D., 2016, A&A, 586, L5
- Kameswara Rao, N.K. and Reddy, B.E., 2005, MNRAS, 357, 235
- Lambert, D.L., Hinckel, K.H. and Luck, R.L., 1988, ApJ, 333, 917
- Lloyd Evans, T., 1985, MNRAS, 217, 493
- Luck, R.E. and Bond, H.E., 1984, ApJ, 279, 729
- Maas, T., Van Winckel, H., Lloyd Evans, T. 2005, A&A, 429, 297
- Marshall, D.J., Robin, A.C., Reyle, C., Schultheis, M. and Picaud, S., 2006, A&A, 453, 653
- Mathis, J.S. and Lamers, H.J.G.L.M., 1992, A&A, 259, L39
- Manick, R., Van Winckel, H., Kamath, D., Hillen, M. and Escorza, A. 2017, A&A, 597, 129
- Manick, R., Van Winckel, H., Kamath, D., Sekaran, S. and Kolenbergh, K. 2018, A&A, 618, 21
- Oomen, Glenn-Michael, Van Winckel, H., Pols, O., and Nelemans, G. 2019, A&A, 629, 49
- Preston, G. W., Krzeminski, W., Smak, J., Williams, J. A. 1963, ApJ, 137, 401
- Reyniers, M., van de Steene, G.C., van Hoof, P.A.M. *et al.* 2007, A&A, 471, 247
- Rao, S.S., Giridhar, S., Lambert, D. L. 2012, MNRAS, 419, 1254
- Sears, F.H., Haynes, E.H., 1908, Laws Observatory Bulletin, University of Missouri, vol. 1, no. 14, 215
- Takeuti, M. and Peterson, J.O., 1983, A&A, 117, 353
- Van Aarle, E., Van Winckel, H., De Smeldt, K. *et al.* 2013, A&A, 554, 106
- van der Bilt, J., 1916, Recherches astronomiques de l'Observatoire d'Utrecht, 6, 139
- Van Winckel, H., 1995, The chemical composition of optically bright post-AGB stars, Ph.D. thesis, K.U. Leuven
- Van Winckel, H. 1997, A&A, 319, 561
- Van Winckel, H. 2003, ARA&A, 41, 391
- Van Winckel, H., Hrivnak, B. J., Gorlova, N., Gielen, C., Lu, W. 2012, A&A, 542, A53
- Van Winckel, H., *et al.* 2009, A&A, 505, 1221
- Vassiliadis, E., Wood, P.R., 1994, ApJS, 92, 125
- Venn, K.A. and Lambert, D.L., 1990, ApJ, 363, 234
- Wallerstein, G. 2002, PASP, 114, 689
- Waters, L.B.F.M., Trams, N.R. and Waelkens, C., 1992, A&A, 262, L37
- Waelkens, C., Van Winckel, H., Bogaert, E., Trams, N. R. 1991